EurJIC
European Journal of Inorganic Chemistry

Full Papers
doi.org/10.1002/ejic.202100125

Chemistry Europe
European Chemical Societies Publishing



# A Cancer Stem Cell Potent Copper(II) Complex with a *S*, *N*, *S*-Schiff base Ligand and Bathophenanthroline

Joshua Northcote-Smith[+],[a] Pooja Kaur[+],[b] and Kogularamanan Suntharalingam*[a]

We investigate the anti-cancer stem cell (CSC) properties of two copper(II) complexes containing 4,7-diphenyl-1,10-phenanthroline and a *S*, *N*, *X*-Schiff base ligand, where X = O (**1**) or S (**2**). Complex **1** was previously reported by us, and is the first metal complex to induce cytotoxic and immunogenic cell death of breast CSCs. Complex **2** is a structural analogue of **1**, where the phenolate moiety (within the Schiff base ligand) is replaced by a thiophenolate group. Complex **2** kills bulk breast cancer cells and breast CSCs in the sub-micromolar range, with reduced toxicity towards non-cancerous epithelial breast cells. Remarkably, **2** is over 10-fold more potent towards breast CSC spheroids than salinomycin (an established anti-breast CSC agent) and cisplatin (a clinically approved anticancer drug). Complex **2** readily enters breast CSCs, accumulates in the cytosol, and increases intracellular reactive oxygen species (ROS) levels upon short exposure (1 h). The latter is likely to be the mechanism by which **2** induces breast CSC death.

## Introduction

Cancer is a dynamic disease with a diverse makeup of cells.[1] Cancer heterogeneity is widely thought to be the underlying reason for therapy resistance.[2] The existence of sub-populations of cancer cells with distinct molecular signatures and varying degrees of treatment responses means current therapeutic regimens are not always completely effective (in the short and long term).[1] Treatment-resistant sub-populations of cancer cells are heavily linked to cancer relapse and metastasis, the leading cause of cancer-related deaths.[3] Cancer stem cells (CSCs) are a genetically distinct subset of tumour cells that can survive traditional cancer treatments (chemotherapy, radiation, and surgery) and generate a progeny of differentiated cancer cells, leading to cancer regeneration.[4] Therefore, for durable clinical outcomes, it is essential that treatment regimens are able to remove entire populations of cancer cells, including hard-to-kill CSCs that can re-seed tumours post-treatment. At present, several academic- and pharmaceutical-led drug discovery programs are underway aimed at developing clinically viable anti-CSC agents.[5] Despite rapid progress in this area over the last decade, a clinically approved anti-CSC agent remains elusive.

Over the last seven years we and others have attempted to utilise the physical and chemical properties offered by metals to develop inorganic anti-CSC agents.[6] Our research, which is conducted primarily at the fundamental bench-side level (compound design, synthesis, and *in vitro* testing), has led to the identification of a promising class of anti-breast CSC agents, namely copper(II) complexes bearing polypyridyl and/or Schiff base ligands.[7] This family of copper(II) complexes kill breast CSCs by elevating intracellular reactive oxygen species (ROS) levels, activating the JNK and p38 stress pathways, and caspase-dependent apoptosis.[7] The high breast CSC potency and selectivity (over bulk breast cancer cells and normal breast cells) of these copper(II) complexes is believed to be due, in part, to the susceptibility of breast CSCs to subtle changes in their redox state.[8]

It should be noted that copper(II) coordination complexes have been widely investigated as anticancer agents for decades.[9] According to the large body work already published on the anticancer properties of copper(II) coordination complexes, cancer cell toxicity and its associated mechanism of action is highly dependent on the coordinating ligands.[9a,b] Despite these efforts, no copper(II) coordination complex has been approved for clinical use in humans as an anticancer drug. The most advanced copper(II) complexes, called Casiopeinas, are currently in Phase I clinical trials.[10] Some of the latest studies suggest that Casiopeinas may be limited by dose-dependent cardiotoxicity,[11] perhaps due to speciation. In the context of the current investigation, it is important to highlight that almost all of the reported studies on the anticancer properties of copper(II) coordination complexes (to date) have focused on bulk cancer cell potency only. Very few studies have reported the effect of copper(II) coordination complexes on hard-to-kill tumour sub-populations such as CSCs.

Recently, we reported a charged copper(II) complex **1**, comprising of a *S*, *N*, *O*-Schiff base ligand $\mathbf{L}^1$ (with oxygen,

[a] *J. Northcote-Smith,[+] Dr. K. Suntharalingam*
*School of Chemistry*
*University of Leicester*
*Leicester, UK*
*E-mail: k.suntharalingam@leicester.ac.uk*
[b] *P. Kaur[+]*
*Department of Immunology and Inflammation*
*Imperial College London*
*London, UK*

[+] *These authors contributed equally to this work.*

*Supporting information for this article is available on the WWW under https://doi.org/10.1002/ejic.202100125*

*Part of the joint "Metals in Medicine" Special Collection with ChemMedChem.*

nitrogen, and sulphur donor atoms) and 4,7-diphenyl-1,10-phenanthroline capable of killing breast CSCs via cytotoxic and immunogenic pathways (see Figure 1 for chemical structures of $\mathbf{L^1}$ and **1**).[12] Copper(II) complex **1** was the first metal complex to evoke immunogenic cell death (ICD) of breast CSCs and stimulate their engulfment by immune cells (macrophages). This was a significant step in our quest to develop clinically viable anti-breast cancer drug candidates, as the eradication of CSCs by immunological pathways could serve as an effective method to remove residual CSCs after conventional bulk cancer cell specific treatments. In this study we explore the breast CSC activity of a structurally related copper(II) complex **2** where the coordinated Schiff base ligand has been subtly modified. Specifically, a thiol moiety was incorporated into the *S*, *N*, *S*-Schiff base ligand scaffold (replacing the hydroxyl moiety in $\mathbf{L^1}$) to yield $\mathbf{L^2}$ which was used to prepare the corresponding copper(II) complex with 4,7-diphenyl-1,10-phenanthroline, **2** (Figure 1, Scheme S1). This synthetically challenging modification was expected to modulate stability in physiologically relevant solutions, intracellular ROS generation, and breast CSC uptake. Herein we report the synthesis, characterisation, and *in vitro* anti-breast CSC properties of the copper(II) complex **2**.

## Results and Discussion

### Synthesis and characterisation

The copper(II) complex **2** was prepared as outlined in Scheme S1. First, the *S*, *N*, *S*-Schiff base ligand $\mathbf{L^2}$ was prepared by reacting equimolar amounts of 2-mercaptobenzaldehyde (prepared using a previously reported protocol)[13] with 2-(methylthio)ethan-1-amine in THF for 16 h under reflux. The ligand $\mathbf{L^2}$ was isolated in a reasonable yield (63%) as a yellow-orange oil and characterised by $^1$H NMR spectroscopy and atmospheric pressure ionization (API) mass spectrometry (see Electronic Supporting Information, Scheme S1, Figures S1-2). The characteristic signal at 8.64 ppm in the $^1$H NMR spectrum of $\mathbf{L^2}$ confirmed formation of the imine functionality. Furthermore, disappearance for the aldehyde proton signal (at 10.23 ppm) corresponding to 2-mercaptobenzaldehyde established full conversion to the imine product (Figure S3). A molecular ion peak corresponding to $\mathbf{L^2}$ was observed in the API-MS (negative mode) ($m/z = 211.7$ $[\mathbf{L^2}]^-$; Figure S2) with no trace of the molecular ion peak for the starting material, 2-mercaptobenzaldehyde ($m/z = 137.0$ $[M–H]^-$; Figure S4), further supporting full conversion to the imine product. The copper(II) complex **2** was prepared by reacting equimolar amounts of 4,7-diphenyl-1,10-phenanthroline with copper(II) nitrate hydrate in methanol, followed by the addition of $\mathbf{L^2}$ and leaving the resultant solution stirring at room temperature for 16 h (Scheme S1). Excess sodium hexafluorophosphate was then added to isolate **2** in the monocationic form as a green solid. The copper(II) complex **2** was characterised by high-resolution ESI mass spectrometry and elemental analysis (see Electronic Supporting Information, Figure S5). A distinctive molecular ion peak corresponding to **2** with the appropriate isotopic pattern was observed in the HR-ESI MS ($m/z = 772.2086$ $[\mathbf{2}\text{-H} + \text{Na}]^+$; Figure S5). The purity of **2** was established by elemental analysis (see Electronic Supporting Information).

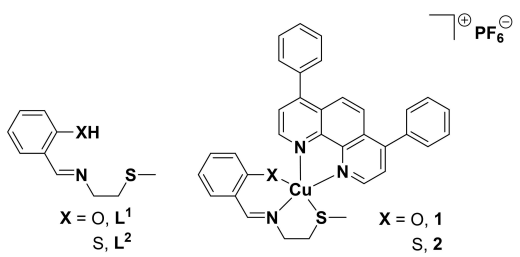


**Figure 1.** Chemical structures of the Schiff base ligands $\mathbf{L^1}$ and $\mathbf{L^2}$, and the corresponding copper(II) complexes **1** and **2** containing $\mathbf{L^1}$ or $\mathbf{L^2}$ and 4,7-diphenyl-1,10-phenanthroline.

### Lipophilicity and solution stability

Lipophlicity is an important biophysical property for small molecule therapeutics as it directly influences absorption, distribution, cellular uptake, and toxicity.[14] The lipophilicity of **2** was determined by measuring the extent to which it partitioned between octanol and water, P. The experimentally determined LogP value for **2** was $0.13 \pm 0.03$. The amphiphilic nature of **2** suggests that it should be partially soluble in aqueous solutions and readily taken up by cells. The experimentally determined LogP value for **1** was $2.01 \pm 0.16$, suggesting that replacement of the copper(II)-coordinating oxygen atom in **1** for a sulphur atom in **2** markedly increases hydrophilicity. UV-Vis and $^1$H NMR spectroscopy, and high-resolution ESI mass spectrometry studies were carried out to assess the integrity of **2** in biologically relevant solutions. In PBS:DMSO (200:1), the absorbance of the π-π* and MLCT bands associated to **2** (25 μM) decreased by up to 65% over the course of 24 h at 37 °C (Figure S6). Nevertheless, the wavelengths associated to the π-π* and MLCT bands for **2** (25 μM) remained unaltered, indicative of reasonable stability under these conditions (Figure S6). In PBS:DMSO (200:1) in the presence of ascorbic acid (10 equivalents), a cellular reductant, the absorbance of the UV-Vis trace for **2** (25 μM) decreased by up to 43% over the course of 24 h at 37 °C (Figure S7). Upon addition of bathocuproine disulfonate (BCS, 2 equivalents), a strong copper(I) chelator, to a PBS:DMSO (200:1) solution of **2** (50 μM) and ascorbic acid (10 equivalents), a characteristic absorbance band at 480 nm corresponding to $[Cu^I(BCS)_2]^{3-}$ was observed (Figure 2A), suggestive of reduction of the copper(II) centre in **2** to copper(I).[15] Taken together, the UV-Vis spectroscopy studies indicate that **2** is reduced from the copper(II) to copper(I) form under biologically reducing conditions. The HR-ESI (positive) mass spectrum of **2** (500 μM) in the presence of ascorbic acid (10 equivalents), in $H_2O$:DMSO (10:1) was dominated by a molecular ion peak corresponding to $[Cu^I(4,7\text{-diphenyl-1,10-phenanthroline})_2]^+$ (727.1896 *m/z*) with the appropriate isotopic pattern (Figure 2B). This suggests that the copper(II) centre in **2** undergoes reduction to copper(I), triggering ligand exchange.

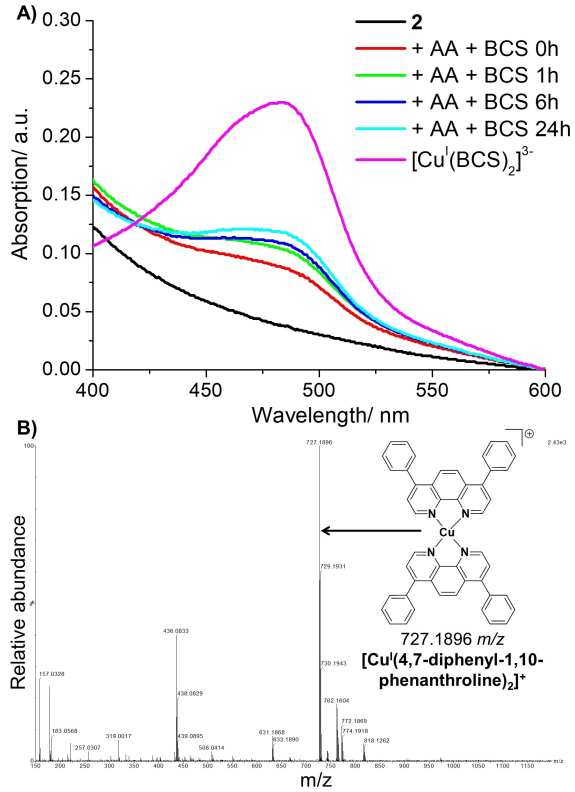


**Figure 2.** (A) UV-Vis spectrum of **2** (50 μM) in the presence of ascorbic acid (500 μM) and bathocuproine disulfonate, BCS (100 μM) in PBS:DMSO (200:1) over the course of 24 h at 37 °C. (B) High resolution ESI mass spectrum (positive mode) of **2** (500 μM) in $H_2O$:DMSO (10:1) in the presence of ascorbic acid (5 mM) after 24 h incubation at 37 °C.

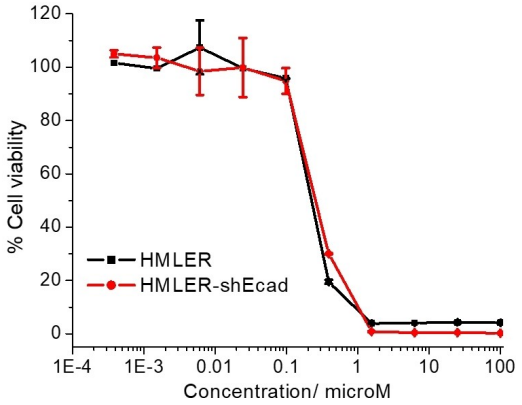


**Figure 3.** Representative dose-response curves for the treatment of HMLER and HMLER-shEcad cells with **2** after 72 h incubation.

**Table 1.** $IC_{50}$ values of the copper(II) complexes **1** and **2**, cisplatin, and salinomycin, against HMLER cells, HMLER-shEcad cells, and HMLER-shEcad mammospheres.

| Compound | HMLER $IC_{50}$ [μM][a] | HMLER-shEcad $IC_{50}$ [μM][a] | Mammosphere $IC_{50}$ [μM][b] |
|---|---|---|---|
| **1**[c] | 0.21 ± 0.01 | 0.32 ± 0.02 | 0.54 ± 0.01 |
| **2** | 0.22 ± 0.01 | 0.25 ± 0.01 | 1.26 ± 0.04 |
| cisplatin [c] | 2.57 ± 0.02 | 5.65 ± 0.30 | 13.50 ± 2.34 |
| salinomycin [c] | 11.43 ± 0.42 | 4.23 ± 0.35 | 18.50 ± 1.50 |

[a] Determined after 72 h incubation (mean of three independent experiments ± SD). [b] Determined after 5 days incubation (mean of three independent experiments SD). [c] Reported in references 7a, 7d, 12, and 16.

The $^1$H NMR spectrum of **2** (1 mM) in DMSO-$d_6$:$D_2O$ (10:1) displayed broad peaks, typical of a paramagnetic copper(II) complex (Figure S8A). The $^1$H NMR spectrum of **2** (1 mM) in the presence of ascorbic acid (1 mM) in DMSO-$d_6$:$D_2O$ (10:1) displayed well defined peaks, consistent with the formation a diamagnetic copper(I) species (Figure S8B). Signals in the aromatic region of the $^1$H NMR spectrum can be tentatively assigned to $[Cu^I(4,7\text{-diphenyl-1,10-phenanthroline})_2]^+$. The ESI mass spectrum of the DMSO-$d_6$:$D_2O$ (10:1) solution clearly displayed the molecular ion peak corresponding to $[Cu^I(4,7\text{-diphenyl-1,10-phenanthroline})_2]^+$ (727 *m/z*) with the appropriate isotopic pattern (Figure S9). These studies indicate that the copper(II) centre in **2** undergoes reduction to copper(I) in the presence of ascorbic acid. It should be noted that although the copper(I) form detected under the conditions used in the abovementioned experiments is $[Cu^I(4,7\text{-diphenyl-1,10-phenanthroline})_2]^+$ it is unlikely to be the major reduced product formed in cells given the high intracellular concentration (millimolar range) of nitrogen- and sulphur-containing biological nucleophiles with high copper(I) affinities. Such biomolecules are likely to outcompete 4,7-diphenyl-1,10-phenanthroline for copper(I) inside cells. Prior to preforming cellular studies, the stability of **2** (25 μM) was gauged in mammary epithelial cell growth medium (MEGM) (at 37 °C over the course of 24 h) using UV-Vis spectroscopy (Figure S10). Complex **2** was deemed to be reasonably stable under these conditions.

## Monolayer and mammosphere CSC potency

The cytotoxicity of the copper(II) complex **2** towards bulk breast cancer cells (HMLER) and breast CSCs (HMLER-shEcad) in monolayer cultures was assessed using the colorimetric MTT assay. $IC_{50}$ values were determined from dose-response curves (Figure 3) and are shown in Table 1. The copper(II) complex **2** exhibited equal potency towards HMLER and HMLER-shEcad cells, within the sub-micromolar range (Table 1). This implies that **2** has the potential to kill entire heterogeneous breast cancer cell populations (consisting of bulk breast cancer cells and breast CSCs) with a single sub-micromolar dose. The $IC_{50}$ values of **2** towards HMLER and HMLER-shEcad cells were similar to the parent copper(II) complex **1**,[12] indicating that replacement of the phenolate group in **1** with a thiophenolate group in **2**, does not detrimentally effect potency towards bulk breast cancer cells and breast CSCs. Notably, the potency of **2** towards breast CSC-enriched HMLER-shEcad cells was 17-and 23-fold greater than that of salinomycin (a clinically tested anti-breast CSC agent) and cisplatin (a clinically approved platinum-based anticancer agent), respectively (Table 1).[7a,16] To gauge therapeutic potential, the cytotoxicity of **2** towards non-cancer-

ous epithelial breast MCF10A cells was determined. The copper (II) complex **2** was less potent towards MCF10A cells than HMLER and HMLER-shEcad cells ($IC_{50}$ value = 0.51 ± 0.01 μM, up to 2.3-fold, $p < 0.05$) (Figure S11). Therefore, according to the cytotoxicity studies in monolayer systems, **2** has the potential to preferentially kill breast CSCs and bulk breast cancer cells over non-cancerous breast cells at certain sub-micromolar concentrations.

To provide more clinically relevant potency data, mammosphere studies were performed. When CSCs are cultured in serum-free media, under low-attachment conditions, three-dimensional spheroids representative of tumours are formed.[17] These structures provide a reliable *in vitro* model to probe CSC activity. The ability of **2** (at a non-lethal dose) to inhibit HMLER-shEcad mammosphere formation from single cell suspensions was determined using an inverted microscope. Treatment of HMLER-shEcad cells with **2** (at the $IC_{20}$ value after 5 days incubation) significantly reduced ($p < 0.05$) the number and size of mammospheres formed (Figure 4A, Figure 4B). A comparable result was observed for salinomycin (Figure 4A, Figure 4B) under identical conditions. More specifically, **2** reduced the number of mammospheres formed by 48% compared to the untreated control, whereas salinomycin induced a 54% reduction in the number of mammospheres formed. It should be noted that the parent copper(II) complex **1** induced a 74% reduction in the number of mammospheres formed compared to the untreated control under identical conditions.[12] To determine the ability of **2** to reduce mammosphere viability, TOX8 a resazurin-based reagent was used.[18] The $IC_{50}$ value of **2** (the concentration of **2** required to reduce mammosphere viability by 50%) was extrapolated from a dose-response curve (Figure S12) and is shown in Table 1. The $IC_{50}$ value for **2** was in the low micromolar range. The mammosphere potency of **2** was 14.7-and 10.7-fold greater than salinomycin and cisplatin, respectively (Table 1), and 2.3-fold lower than **1**.[7d,12,16] Overall, the mammosphere studies show that **2** is able to markedly reduce mammosphere formation, size, and viability, however its mammosphere inhibitory effect was somewhat reduced compared to the parent copper(II) complex **1**.

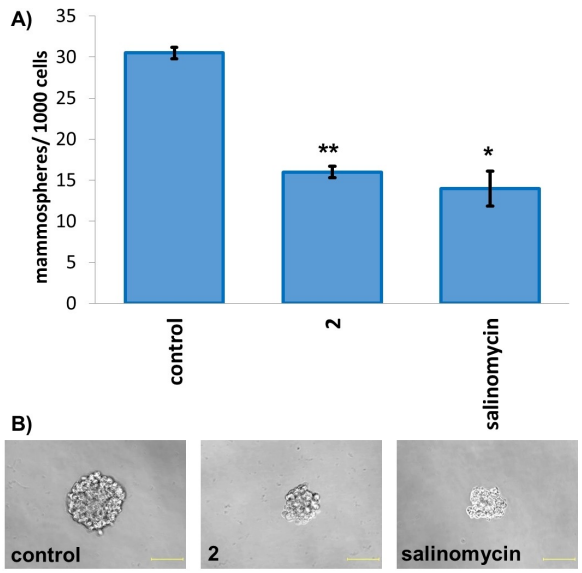


**Figure 4.** (A) Representation of the number of mammospheres formed from HMLER-shEcad cell suspensions treated with **2** or salinomycin for 5 days at their respective $IC_{20}$ values. Error bars = SD and Student t-test, * = $p < 0.05$, ** = $p < 0.01$. (B) Bright-field images (taken using an inverted microscope) representative of untreated HMLER-shEcad mammospheres and those treated with **2** or salinomycin for 5 days at their respective $IC_{20}$ values. Scale bar = 100 μm.

### Insight into the mechanism of CSC cytotoxicity

Cellular uptake studies were carried out to determine the bulk breast cancer cell and breast CSC permeability of **2**. HMLER and HMLER-shEcad cells were independently incubated with **2** (5 μM for 24 h) and the intracellular copper content was determined by inductively coupled plasma mass spectrometry (ICP-MS). Identical studies were also carried out with **1** (5 μM for 24 h) for comparison. Both copper(II) complexes, **2** (495.0 ± 0.3 to 525.7 ± 1.3 ng of Cu/ million cells) and **1** (465.5 ± 1.0 to 482.3 ± 2.1 ng of Cu/ million cells) were readily internalised by HMLER and HMLER-shEcad cells. The similar level of HMLER and HMLER-shEcad cell uptake of **1** and **2** is consistent with their comparable potencies towards the respective cell lines (Table 1). Collectively, the cellular uptake data shows that the slight structural modification between **2** and **1** does not markedly affect bulk breast cancer cell or breast CSC uptake. Fractionation studies with HMLER-shEcad cells treated with **2** (5 μM for 24 h) indicated that 65% (341.7 ng of Cu/million cells) of internalised **2** was detected in the cytoplasm, with only 7% (36.8 ng of Cu/million cells) found in the nucleus. The remainder of **2** that was absorbed by HMLER-shEcad cells was observed in the cell membrane fraction. This suggests that the cellular targets of **2** are likely to be biomolecules residing in the cytosol rather than nucleus-housed biomolecules such as genomic DNA or histone proteins.

Copper(II) complexes compromising of Schiff base and/or 4,7-diphenyl-1,10-phenanthroline ligands are known to induce CSC death by generating ROS.[7b–d] Indeed, we have previously shown that **1** induces breast CSC apoptosis by increasing ROS levels within the endoplasmic reticulum.[12] To determine if **2**-induced breast CSC cytotoxicity is associated to ROS generation, intracellular ROS levels were measured over the course of 48 h using 6-carboxy-2′,7′-dichlorodihydrofluorescein diacetate (DCFH-DA), a well-established ROS indicator. HMLER-shEcad cells dosed with **2** ($IC_{50}$ value) displayed a significant increase in ROS levels relative to untreated control cells after 1 h exposure (45% increase, $p < 0.05$) (Figure S13). Prolonged (3–48 h) exposure of **2** did not increase intracellular ROS levels to the same extent, although a statistically insignificant increase ($p > 0.05$) in ROS levels was observed after 3 and 16 h exposure. Taken together, this suggests that HMLER-shEcad cells dosed with **2** experience a sharp ROS burst within the first hour of exposure and then ROS levels attenuate to levels observed in untreated control cells. Similar time-dependent ROS generation properties have been previously reported for **1** and other CSC-potent copper(II) complexes.[7c,d,12] The ROS studies also suggest that **2**-

induced breast CSC death could be associated to intracellular ROS generation. To corroborate this, independent cell viability studies were carried out in the presence of *N*-acetylcysteine (2 mM, 72 h), a ROS scavenger. In the presence of *N*-acetylcysteine the potency of **2** towards HMLER-shEcad cells decreased significantly ($IC_{50}$ value increased 8.8-fold to 2.21 ± 0.17 μM, $p < 0.05$) (Figure S14). Overall, the ROS and cytotoxicity studies indicate that **2**-mediated breast CSC death is likely to be related to intracellular ROS production.

## Conclusion

In summary, we report the synthesis, spectroscopic and analytical characterisation, and *in vitro* anti-breast CSC properties of a copper(II) complex, **2**, consisting of a Schiff base ligand (with two sulphur and one nitrogen donor atoms) and 4,7-diphenyl-1,10-phenanthroline. Akin to the parent copper(II) complex **1**, **2** simultaneously kills bulk breast cancer and breast CSCs in the sub-micromolar range, which implies that **2** has the potential to remove heterogenous breast tumour populations (containing bulk breast cancer cells and breast CSCs) with a single (sub-micromolar) dose. Studies in three-dimensional CSC cultures indicate that **2** is over one order of magnitude more potent towards mammospheres than salinomycin and cisplatin. Cellular uptake studies show that **2** was internalised by breast CSCs to a similar extent as **1**, and localized predominately in the cytoplasm. Furthermore, **2** is able to generate significant levels of intracellular ROS (45% increase relative to untreated control breast CSCs) after a short exposure time (1 h), and this may be the mechanism by which it induces breast CSC death. Overall, the results presented in this study further highlight the promising anti-CSC properties of redox-modulating copper(II) complexes containing Schiff base and phenanthroline ligands. We believe that these findings justify the continued development of this class of redox-active metal complexes as potential CSC-directed chemotherapeutics. Given our previous work on the cytotoxic and immunogenic properties of the parent copper (II) complex **1**, our future work with **2** will focus on determining the detailed mechanism of CSC death induced by **2** and the ability of **2** to induce immunogenic CSC death.

## Experimental Section

**Materials and Methods**. All synthetic procedures were performed under normal atmospheric conditions or under nitrogen. High-resolution electron spray ionisation mass spectra were obtained by Dr Lisa Haigh (Imperial College London) on a Bruker Daltonics Esquire 3000 spectrometer. Atmospheric pressure ionization mass spectra were obtained on an Advion Expression compact mass spectrometer with Plate Express and Atmospheric Solids Analysis Probe (ASAP). Elemental analysis was performed commercially by London Metropolitan University. 2-(methylthio)ethan-1-amine, 4,7-diphenyl-1,10-phenanthroline, copper(II) nitrate hydrate, and sodium hexafluorophosphate were purchased from Sigma and used as received. 2-Mercaptobenzaldehyde was prepared according to a previously reported protocol.[13]

**Synthesis of $L^2$**. 2-Mercaptobenzaldehyde (254.7 mg, 1.8 mmol) and 2-(methylthio)ethan-1-amine (185.5 mg, 2.0 mmol) was refluxed in THF (20 mL) for 16 h. The reaction mixture was then reduced under vacuum to afford $L^2$ as a yellow-orange oil (246.0 mg, 63%); $^1$H NMR (400 MHz, $CDCl_3$): δ 8.64 (s, 1H, N=C*H*), 7.76 (dd, 1H, Ar–*H*), 7.70 (dd, 1H, Ar–*H*), 7.32–7.28 (m, 2H, Ar–*H*), 3.85 (t, 2H, C$H_2$), 2.86 (t, 2H, C$H_2$), 2.17 (s, 3H, C$H_3$); API-MS (negative) Calcd. for $C_{10}H_{13}NS_2$ $[L^2]^-$ 211.3 a.m.u. Found $[L^2]^-$: 211.7 a.m.u.

**Synthesis of $[Cu^{II}(L^2)$(4,7-diphenyl-1,10-phenanthroline)$][PF_6]$, 2**. $Cu(NO)_2 \cdot 3H_2O$ (126.1 mg, 0.5 mmol) and 4,7-diphenyl-1,10-phenanthroline (172.3 mg, 0.5 mmol) were dissolved in methanol (18 mL) and the resultant blue solution was stirred for 30 min at room temperature. $L^2$ (108.8 mg, 0.5 mmol) in methanol (8 mL) was then added dropwise, and the green reaction mixture was stirred for 16 h at room temperature. $NaPF_6$ (190.1 mg, 1.1 mmol) was added and the reaction mixture was stirred at room temperature for 10 min. The resulting precipitate was filtered, washed thoroughly with cold methanol (10 mL) and diethyl ether (10 mL), and dried to obtain **2** as a green solid (14.0 mg, 4%); HRMS (ESI) (DMSO) Calcd. for $C_{34}H_{27}CuF_6N_3PS_2Na$ [**2**-H + Na]$^+$: 772.6647 a.m.u., Found: [**2**-H + Na]$^+$: 772.2086 a.m.u.; EA Anal. Calcd. for **2** ($C_{34}H_{28}CuF_6N_3PS_2$): C, 54.36; H, 3.76; N, 5.59. Found: C, 54.53 ; H, 3.51; N, 5.48.

**Measurement of water-octanol partition coefficient (LogP)**. The LogP value for **2** was determined using the shake-flask method. The 1-octanol used in this experiment was pre-saturated with water. An aqueous solution of **2** (500 μL, 100 μM) was incubated with 1-octanol (500 μL) in a 1.5 mL tube. The tube was shaken at room temperature for 24 h. The two phases were separated by centrifugation and the concentration of **2** in the water and 1-octanol layer was determined by UV-Vis spectroscopy. The LogP value for **1** was previously reported by us in reference 12.

**Cell Lines and Cell Culture Conditions**. The human mammary epithelial cell lines, HMLER and HMLER-shEcad were kindly donated by Prof. R. A. Weinberg (Whitehead Institute, MIT). The human epithelial breast MCF10A cell line was acquired from the American Type Culture Collection (ATCC, Manassas, VA, USA). HMLER, HMLER-shEcad, and MCF10A cells were maintained in Mammary Epithelial Cell Growth Medium (MEGM) with supplements and growth factors (BPE, hydrocortisone, hEGF, insulin, and gentamicin/amphotericin-B). The cells were grown at 310 K in a humidified atmosphere containing 5% $CO_2$.

**Cytotoxicity MTT assay**. The colorimetric MTT assay was used to determine the toxicity of **2**. HMLER, HMLER-shEcad, or MCF10A cells ($5 \times 10^3$) were seeded in each well of a 96-well plate. After incubating the cells overnight, various concentrations of **2** (0.0004–100 μM), were added and incubated for 72 h (total volume 200 μL). A stock solution of **2** (10 mM) was prepared in DMSO and diluted using media. The final concentration of DMSO in each well did not exceed 1% and this amount was present in the untreated control as well. After 72 h, 20 μL of a 4 mg/mL solution of MTT in PBS was added to each well, and the plate was incubated for an additional 4 h. The MEGM/MTT mixture was aspirated and 200 μL of DMSO was added to dissolve the resulting purple formazan crystals. The absorbance of the solutions in each well was read at 550 nm. Absorbance values were normalized to (DMSO-containing) control wells and plotted as concentration of test compound versus % cell viability. $IC_{50}$ values were interpolated from the resulting dose dependent curves. The reported $IC_{50}$ values are the average of three independent experiments, each consisting of six replicates per concentration level (overall n = 18).

**Mammosphere Formation and Viability Assay**. HMLER-shEcad cells ($5 \times 10^3$) were plated in ultralow-attachment 96-well plates (Corning) and incubated in MEGM supplemented with B27 (Invitrogen),

20 ng/mL EGF, and 4 μg/mL heparin (Sigma) for 5 days. Studies were also conducted in the presence of **2** and salinomycin (0–133 μM). Spheroids treated with **2** and salinomycin (at their respective $IC_{20}$ values, 5 days) were counted and imaged using an inverted microscope. The viability of the spheroids was determined by addition of a resazurin-based reagent, TOX8 (Sigma). After incubation for 16 h, the solutions were carefully transferred to a black 96-well plate (Corning), and the fluorescence of the solutions was read at 590 nm ($\lambda_{ex}$ = 560 nm). Viable spheroids reduce the amount of the oxidized TOX8 form (blue) and concurrently increase the amount of the fluorescent TOX8 intermediate (red), indicating the degree of spheroid cytotoxicity caused by the test compound. Fluorescence values were normalized to DMSO-containing controls and plotted as concentration of test compound versus % spheroid viability. $IC_{50}$ values were interpolated from the resulting dose dependent curves. The reported $IC_{50}$ values are the average of three independent experiments, each consisting of three replicates per concentration level (overall n = 9).

**Cellular Uptake**. To measure the cellular uptake of **1** and **2**, *ca.* $1\times10^6$ HMLER and HMLER-shEcad cells were independently treated with **1** and **2** (5 μM) at 37 °C for 24 h. After incubation, the media was removed and the cells were washed with PBS (2 mL × 3), and harvested. The number of cells was counted at this stage, using a haemocytometer. This mitigates any cell death induced by **1** and **2** at the administered concentration and experimental cell loss. The cells were centrifuged to form pellets. The cellular pellets were dissolved in 65% $HNO_3$ (250 μL) overnight. A pellet of **2** treated HMLER-shEcad cells was also used to determine the copper content in the nuclear, cytoplasmic, and membrane fractions. The Thermo Scientific NE-PER Nuclear and Cytoplasmic Extraction Kit was used to extract and separate the nuclear, cytoplasmic, and membrane fractions. The fractions were dissolved in 65% $HNO_3$ overnight (250 μL final volume). All samples were diluted 5-fold with water and analysed using inductively coupled plasma mass spectrometry (ICP-MS, PerkinElmer NexION 350D). Copper levels are expressed as Cu (ng) per million cells. Results are presented as the mean of five determinations for each data point.

**Intracellular ROS Assay**. HMLER-shEcad cells ($5\times10^3$) were seeded in each well of a 96-well plate. After incubating the cells overnight, they were treated with **2** ($IC_{50}$ value for 1–48 h) and incubated with 6-carboxy-2′,7′-dichlorodihydrofluorescein diacetate (20 μM) for 30 min. The intracellular ROS level was determined by measuring the fluorescence of the solutions in each well at 529 nm ($\lambda_{ex}$ = 504 nm).

## Acknowledgements

*K.S. is supported by an EPSRC New Investigator Award (EP/S005544/1).*

## Conflict of Interest

The authors declare no conflict of interest.

**Keywords:** Copper · Cancer stem cells · Bioinorganic chemistry · Antitumour agents · Reactive oxygen species

[1] I. Dagogo-Jack, A. T. Shaw, *Nat. Rev. Clin. Oncol.* **2018**, *15*, 81–94.
[2] N. C. Turner, J. S. Reis-Filho, *Lancet Oncol.* **2012**, *13*, e178–185.
[3] a) J. Marx, *Science* **2007**, *317*, 1029–1031; b) R. A. Burrell, N. McGranahan, J. Bartek, C. Swanton, *Nature* **2013**, *501*, 338–345; c) A. Kreso, J. E. Dick, *Cell Stem Cell* **2014**, *14*, 275–291.
[4] a) J. C. Chang, *Medicine* **2016**, *95*, S20-S25; b) L. V. Nguyen, R. Vanner, P. Dirks, C. J. Eaves, *Nat. Rev. Cancer* **2012**, *12*, 133–143.
[5] a) J. Kaiser, *Science* **2015**, *347*, 226–229; b) F. Y. Du, Q. F. Zhou, W. J. Sun, G. L. Chen, *World J. Stem Cells* **2019**, *11*, 398–420.
[6] a) K. Laws, K. Suntharalingam, *ChemBioChem* **2018**, *19*, 2246–2253; b) A. Johnson, J. Northcote-Smith, K. Suntharalingam, *Trends Chem.* **2021**, *3*, 47–58.
[7] a) J. N. Boodram, I. J. McGregor, P. M. Bruno, P. B. Cressey, M. T. Hemann, K. Suntharalingam, *Angew. Chem. Int. Ed.* **2016**, *55*, 2845–2850; *Angew. Chem.* **2016**, *128*, 2895–2900; b) A. Eskandari, J. N. Boodram, P. B. Cressey, C. Lu, P. M. Bruno, M. T. Hemann, K. Suntharalingam, *Dalton Trans.* **2016**, *45*, 17867–17873; c) C. Lu, A. Eskandari, P. B. Cressey, K. Suntharalingam, *Chem. Eur. J.* **2017**, *23*, 11366–11374; d) C. Lu, K. Laws, A. Eskandari, K. Suntharalingam, *Dalton Trans.* **2017**, *46*, 12785–12789.
[8] a) M. Diehn, R. W. Cho, N. A. Lobo, T. Kalisky, M. J. Dorie, A. N. Kulp, D. Qian, J. S. Lam, L. E. Ailles, M. Wong, B. Joshua, M. J. Kaplan, I. Wapnir, F. M. Dirbas, G. Somlo, C. Garberoglio, B. Paz, J. Shen, S. K. Lau, S. R. Quake, J. M. Brown, I. L. Weissman, M. F. Clarke, *Nature* **2009**, *458*, 780–783; b) X. Shi, Y. Zhang, J. Zheng, J. Pan, *Antioxid. Redox Signaling* **2012**, *16*, 1215–1228.
[9] a) C. Marzano, M. Pellei, F. Tisato, C. Santini, *Anti-Cancer Agents Med. Chem.* **2009**, *9*, 185–211; b) C. Santini, M. Pellei, V. Gandin, M. Porchia, F. Tisato, C. Marzano, *Chem. Rev.* **2014**, *114*, 815–862; c) J. O. Pinho, J. D. Amaral, R. E. Castro, C. M. Rodrigues, A. Casini, G. Soveral, M. M. Gaspar, *Nanomedicine* **2019**, *14*, 835–850.
[10] a) R. Galindo-Murillo, J. C. Garcia-Ramos, L. Ruiz-Azuara, T. E. Cheatham, 3rd, F. Cortes-Guzman, *Nucleic Acids Res.* **2015**, *43*, 5364–5376; b) L. Ruiz-Azuara, M. E. Bravo-Gomez, *Curr. Med. Chem.* **2010**, *17*, 3606–3615; c) G. Vertiz, L. E. Garcia-Ortuno, J. P. Bernal, M. E. Bravo-Gomez, E. Lounejeva, A. Huerta, L. Ruiz-Azuara, *Fundam. Clin. Pharmacol.* **2014**, *28*, 78–87; d) M. Wehbe, A. W. Y. Leung, M. J. Abrams, C. Orvig, M. B. Bally, *Dalton Trans.* **2017**, *46*, 10758–10773; e) G. de Anda-Jáuregui, J. Espinal-Enríquez, J. Hur, S. A. Alcalá-Corona, L. Ruiz-Azuara, E. Hernández-Lemus, *Comput. Biol. Chem.* **2019**, *78*, 127–132; f) J. Serment-Guerrero, P. Cano-Sanchez, E. Reyes-Perez, F. Velazquez-Garcia, M. E. Bravo-Gomez, L. Ruiz-Azuara, *Toxicol. in Vitro* **2011**, *25*, 1376–1384.
[11] C. Silva-Platas, C. A. Villegas, Y. Oropeza-Almazan, M. Carranca, A. Torres-Quintanilla, O. Lozano, J. Valero-Elizondo, E. C. Castillo, J. Bernal-Ramirez, E. Fernandez-Sada, L. F. Vega, N. Trevino-Saldana, H. Chapoy-Villanueva, L. Ruiz-Azuara, C. Hernandez-Brenes, L. Elizondo-Montemayor, C. E. Guerrero-Beltran, K. Carvajal, M. E. Bravo-Gomez, G. Garcia-Rivas, *Oxid. Met.* **2018**, *2018*, 8949450.
[12] P. Kaur, A. Johnson, J. Northcote-Smith, C. Lu, K. Suntharalingam, *ChemBioChem* **2020**, *21*, 3618–3624.
[13] Q. Niu, X. Xu, H. Sun, X. Li, *Chin. J. Chem.* **2012**, *30*, 2495–2500.
[14] M. J. Waring, *Expert Opin. Drug Discovery* **2010**, *5*, 235–248.
[15] A. A. Kumbhar, A. T. Franks, R. J. Butcher, K. J. Franz, *Chem. Commun.* **2013**, *49*, 2460–2462.
[16] A. Eskandari, A. Kundu, S. Ghosh, K. Suntharalingam, *Angew. Chem. Int. Ed.* **2019**, *58*, 12059–12064; *Angew. Chem.* **2019**, *131*, 12187–12192.
[17] G. Dontu, W. M. Abdallah, J. M. Foley, K. W. Jackson, M. F. Clarke, M. J. Kawamura, M. S. Wicha, *Genes Dev.* **2003**, *17*, 1253–1270.
[18] R. Mezencev, L. Wang, J. F. McDonald, *J. Ovarian Res.* **2012**, *5*, 30.

Manuscript received: February 13, 2021
Revised manuscript received: March 13, 2021
Accepted manuscript online: March 15, 2021